

## A Continuous Model Studying T Cell Differentiation and Lymphomagenesis and its Distinction with Discrete Models

GUANYU WANG, GERHARD R. F. KRUEGER and L. MAXIMILIAN BUJA

*Department of Pathology and Laboratory Medicine,  
University of Texas - Medical School, Houston, Texas 77030, U.S.A.*

**Abstract.** *The development of T-lymphocytes (T cells) constitute one of the basic and most vital processes in immunology. Conventional mathematical models, being based on the systems theory, fail to sufficiently distinguish the constituents of thymocytes and are thus of limited significance. On the basis of some well thought-out definitions and concepts, a continuous model was designed to describe T cell maturation in the thymus. A partial differential equation was first derived through the analysis of an infinitesimal element of the flow of thymocytes. A computation scheme was designed to determine the growth field in the thymus based upon available experimental data. The corresponding algorithm proved quite simple. A numerical example is given that focuses on the DN stage of the T cell development. The model opens a window for investigating the thymic microenvironment. The potential of the model in studying lymphomagenesis is discussed.*

T-lymphocytes perform a variety of important functions in immune regulation. The constant production of mature T cells depends upon continuous seeding of the thymus by precursor cells from bone marrow. Their differentiation (driven by more than 70 cytokines, tissue factors) in the thymus, which involves a series of steps associated with distinct changes in their surface phenotype, constitutes one of the basic yet very complex processes of immunology.

In mathematical modeling the studied object is usually treated either as a single entity (or few discrete entities) or as infinitely many microscopic entities distributed along some attribute axis. The former is often called a discrete model and the latter a continuous model. Which one is preferable depends on whether or not diversity plays a

central role. For example, the earth is treated as a particle in celestial mechanics, since there is no difference among its constituents as far as their mechanical properties are concerned. However, when it comes to geology the earth is usually continuously modeled since its geological constituents are quite different.

From this perspective, we concluded that to study T cell differentiation as a continuous model is preferable. On one hand, the action of cytokines is thought to be highly localized (1), with functionally effective concentrations being found only in the vicinity of the interacting producer and responder cells. This intimacy of interaction is enhanced by the directional secretion of cytokines, whereby they are only released in the area of contact between the two cells (2). On the other hand, thymocytes are themselves diverse (manifested mainly by different antigen receptors on their surface) and respond differently to the thymic microenvironment (T-MEV). All in all, the internal differences among thymic constituents should be fully exposed, this being achieved more easily by a continuous model. Moreover, for the study of lymphomagenesis, a continuous model is also preferable. Figure 1 shows a distribution of thymocytes with the hatched part indicating the transformed cells. The figure can be easily obtained based on a continuous model, whereby the cancerous information (the peak) is clearly seen. However, a discrete model may measure the whole cohort aggregately, which cannot reflect the existence of the cancerous cells. Indeed, the hatched area is negligible compared to the total area.

Despite its apparent significance, a good continuous model has yet to be designed. Previous models (3,4) studied the temporal dynamics of only four roughly divided thymic compartments (DN, DP, CD4+ SP, CD8+ SP). The thymus as a whole still remains obscure; the internal differences amongst the constituents of each compartment were indistinguishable; the influences of cytokines have not been studied. In brief, those models were based on a system theory that is too general to represent particular biophysical processes and thus it was difficult to probe into the microscopic world of T cell differentiation. In this paper,

*Correspondence to:* Guanyu Wang, Ph.D., Department of Pathology and Laboratory Medicine, University of Texas-Houston Medical School, 6431 Fannin, MSB 2.246, Houston, TX 77030, U.S.A. Tel: (713) 500-6060, Fax: (713) 500-0730, e-mail: Guanyu.Wang@uth.tmc.edu

*Key Words:* T cell differentiation, mathematical modeling, lymphomagenesis.

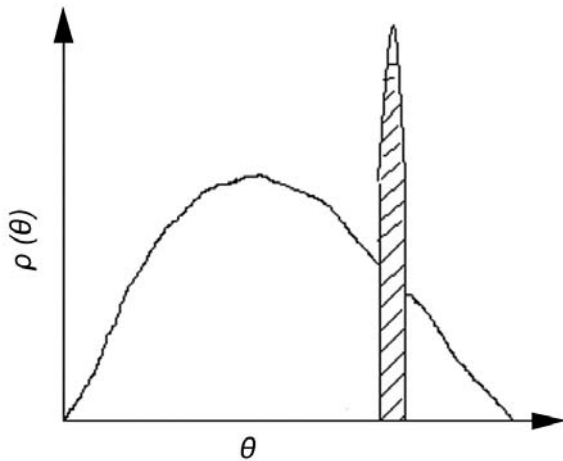


Figure 1. The distribution of a cohort of thymocytes with the hatched area indicating cancerous cells.

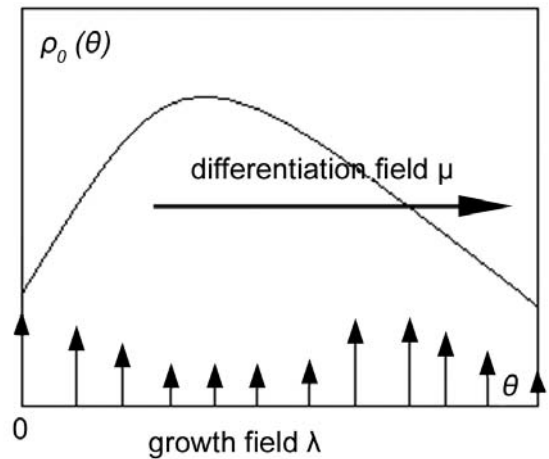


Figure 2. The steady-state distribution of thymocytes sustained by a growth field  $\lambda$  and a differentiation field  $\mu$ .

the complex process is reduced to a tractable, biophysically realistic model by some well thought-out definitions. A general computation scheme is given to determine the model parameters. A numerical example reveals the diverse and rich dynamics manifested by the continuous constituents of the thymic compartments, which were totally ignored by previous models.

**Materials and Methods**

The cohort of thymocytes is thought of in terms of a continuous flow (in contrast to discrete compartments) through the thymus with ever increasing maturity  $\theta$ , initiates as immature stem cells from the bone marrow and ends with mature T cells. On the flow a growth field  $\lambda$  and a differentiation field  $\mu$  are imposed, which represent the total influences of all the cytokines.  $q_0(\theta)$  the steady-state distribution of the cell number, is sustained by the interaction of the two fields (see Figure 2). The dynamic model is derived by the analysis of an infinitesimal element of the flow,  $s=q(\theta,t)d\theta$ , the growth of which is described by  $\frac{\partial s}{\partial t} = \lambda(\theta)s + I - E$ ,

where  $I = q_0 \cdot \mu - \frac{\partial(q \cdot \mu)}{\partial \theta} \frac{d\theta}{2}$  is the influx,  $E = q \cdot \mu + \frac{\partial(q \cdot \mu)}{\partial \theta} \frac{d\theta}{2}$

is the efflux,  $\mu(\theta) = \lim_{\Delta t \rightarrow 0} \frac{\Delta \theta}{\Delta t}$  is the differentiation rate,  $\lambda(\theta) = \lambda^p(\theta) - \lambda^d(\theta)$

is the growth rate that is the difference between the proliferation rate ( $\lambda^p(\theta)$ ) and the death rate ( $\lambda^d(\theta)$ ). Finally one obtains

$$\frac{\partial q(\theta,t)}{\partial t} + \frac{\partial(q(\theta,t)\mu(\theta))}{\partial \theta} = \lambda(\theta)q(\theta,t), \tag{1}$$

with boundary condition  $q(0,t)\mu(0) = I_0$ , where  $I_0$  represents the number of cells to enter the thymus in unit time (one day).  $\theta$  is defined as the maturity of a thymocyte of the healthy animal. It is quantitatively identified with the age of the cell, namely the elapsed time after the cell entered the thymus. For example,  $\theta=0$  represents the maturity

possessed by those cells that are entering the thymus. They then mature linearly with time and by day  $v$  they possess maturity  $\theta=v$ . As a benefit of the definition, the differentiation rate for the healthy state is normalized and has the simple expression  $\mu(\theta) = \lim_{\Delta t \rightarrow 0} \frac{\Delta \theta}{\Delta t} = 1$  (the maturity gained in  $\Delta t$  days is quantitatively still  $\Delta t$ ). Although  $\theta$  is defined in terms of the healthy state, it can be used for the unhealthy state as well. In both cases  $\theta=v$  represents exactly the same level of maturation. However, for the unhealthy animal the age of the thymocytes of maturity  $v$  has the expression  $t = \int_0^v d\theta/\mu(\theta)$ , which does not necessarily equal  $v$  since  $\mu(\theta) = 1$  may not hold. The maturation may be advanced or delayed due to various pathological conditions.

In this paper only the healthy animal is considered, in which case  $q(\theta,t) = q_0(\theta)$  is time-invariant (thymocytes are in homeostasis). Eq. (1) then reduces to  $dq_0(\theta)/d\theta = \lambda(\theta)q_0(\theta)$ , with  $q_0(0) = I_0$ . The primary problem is the inverse problem, namely the determination of  $\lambda(\theta)$  based on the experimental data. To be determined numerically,  $\lambda(\theta) = \sum_{j=1}^N \alpha_j \cdot f_j(\theta)$  is first constructed in a

space that is spanned by some basis functions  $f_j(j=1,2,\dots,N)$ , by which  $q_0(\theta)$  has the expression

$$q_0(\theta) = I_0 \cdot \exp \left( \sum_{j=1}^N \alpha_j \cdot \int_0^\theta f_j(\alpha) d\alpha \right). \tag{2}$$

The experimental data can only be collected discretely, by dividing the whole thymocytes into  $N$  subsets according to certain cell marker expressions. However, the delimitations between these subsets are unknown in terms of the defined maturity, which introduces  $N$  additional unknowns  $\theta = [\theta_1, \theta_2, \dots, \theta_N]^T$  (see Figure 3). Therefore, in total we have  $2N$  unknowns  $\mathbf{x} = [\mathbf{a} \ \boldsymbol{\theta}]^T$ , where  $\mathbf{a} = [a_1, a_2, \dots, a_N]^T$ . To obtain them  $2N$  data have to be found. We use  $\mathbf{S} = [S_1, S_2, \dots, S_N]^T$  and  $\bar{\lambda} = [\bar{\lambda}_1, \bar{\lambda}_2, \dots, \bar{\lambda}_N]^T$ , both of which can be acquired by flow cytometry analysis.  $S_i$  is the cell count of subset  $i$ ;  $\bar{\lambda}_i$  is the growth rate of subset  $i$ . To relate the unknowns  $\mathbf{x}$  to the data  $\mathbf{d} = [\mathbf{S}, \bar{\lambda}]^T$  the following  $2N$  algebraic equations are established,

$$\int_0^{\theta_i} q_0(\theta) d\theta = \sum_{k=1}^i S_k, \quad \text{for } i=1,2,\dots,N, \tag{3}$$

$$\int_{\theta_{i-1}}^{\theta_i} \lambda(\theta) q_0(\theta) d\theta = \bar{\lambda}_i \cdot S_i, \quad \text{for } i=1,2,\dots,N. \tag{4}$$

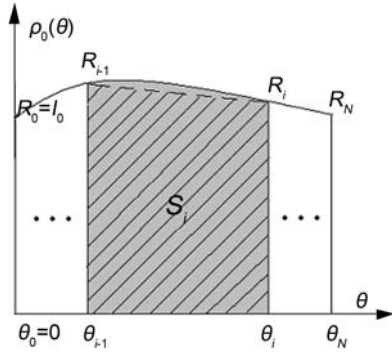


Figure 3. An illustration of parameters  $\theta$ ,  $R$ ,  $S$ .

Eq. (3) is obvious. Eq. (4) is identical with  $\bar{\lambda}_i = \int_{\theta_{i-1}}^{\theta_i} \lambda(\theta) \varrho(\theta) d\theta / \int_{\theta_{i-1}}^{\theta_i} \varrho(\theta) d\theta$ ,

which implies that the aggregatedly measured  $\bar{\lambda}_i$  represents the growth rate averaged over all the cells in subset  $i$ . By using  $\lambda(\theta) \varrho_0(\theta) = d\varrho_0(\theta)/d\theta$ , Eq. (4) reduces to  $\varrho_0(\theta_i) - \varrho_0(\theta_{i-1}) = \bar{\lambda}_i \cdot S_i$ ,  $i=1,2,\dots,N$ , by which  $\varrho_0(\theta_i)$  (denote by  $R_i$  hereinafter) can be sequentially obtained (note that  $\varrho_0(\theta_0) = \varrho_0(0) = I_0$  represents the number of cells to enter the thymus each day, which is known from literature). By replacing  $\theta$  with  $\theta_i$  in Eq. (2), one obtains

$$\sum_{j=1}^N a_j \cdot \int_0^{\theta_i} f_j(a) da - \ln \left( \frac{R_i}{I_0} \right) = 0, \quad \text{for } i, j = 1, 2, \dots, N. \quad (5)$$

Substitute Eq. (2) into Eq. (3), one has

$$I_0 \int_0^{\theta_i} \exp \left( \sum_{j=1}^N a_j \cdot \int_0^{\theta} f_j(a) da \right) d\theta - \sum_{k=1}^i S_k = 0, \quad \text{for } i, j = 1, 2, \dots, N. \quad (6)$$

Eqs. (5-6) are the equations that will actually be used to obtain  $x$ , by Newton's method (5), a standard root-finding method. The method requires the initial trial value be sufficiently close to the actual solution. Therefore a first approximation is necessary.

*First approximation.* From Figure 3 one sees that  $S_i$  (shaded area) approximately equals the hatched trapezoid,  $(\theta_i - \theta_{i-1}) \cdot (R_{i-1} + R_i)/2 \approx S_i$ . Therefore the approximated value  $\theta^{(0)}$  can be obtained according to  $\theta_i^{(0)} = \theta_{i-1}^{(0)} + 2S_i/(R_{i-1} + R_i)$ .  $a^{(0)}$  can subsequently be obtained from Eq. (5) with  $\theta$  replaced with  $\theta^{(0)}$ . The computation is straightforward since Eq. (5) is actually  $\mathbf{a} = \mathbf{Q}^{-1} \cdot \mathbf{b}$ , where  $\mathbf{b} = [\ln(R_1/I_0), \dots, \ln(R_N/I_0)]^T$ ,  $\mathbf{Q}$  is a  $N \times N$  matrix with  $Q_{ij} = \int_{\theta_{i-1}}^{\theta_i} f_j(a) da$ .

*Root finding.*  $\mathbf{x}^{(0)} = [\mathbf{a}^{(0)} \theta^{(0)}]^T$  is then used as the initial value for finding the root of Eqs. (5-6) (denoted by  $F(\mathbf{x}) = 0$  hereinafter). Newton's method is formulated as follows.

$$\begin{aligned} & \text{Given } \mathbf{x}^{(0)}, \text{ for } k=0,1,2,\dots, \text{ until convergence:} \\ & \text{Solve: } J_F(\mathbf{x}^{(k)}) \delta \mathbf{x}^{(k)} = F(\mathbf{x}^{(k)}), \\ & \text{Set: } \mathbf{x}^{(k+1)} = \mathbf{x}^{(k)} - \delta \mathbf{x}^{(k)}, \end{aligned}$$

where  $J_F(\mathbf{x})$  is the Jacobian matrix associated with  $F(\mathbf{x})$ . One can check that  $J_F = \begin{bmatrix} \mathbf{Q} & \mathbf{L} \\ \mathbf{M} & \mathbf{R} \end{bmatrix}$ , where  $\mathbf{L} = \text{diag}\{\lambda(\theta_1), \lambda(\theta_2), \dots, \lambda(\theta_N)\}$   $\mathbf{M}$  is a  $N \times N$

matrix with  $M_{ij} = \int_0^{\theta_i} \varrho_0(\theta) \int_0^{\theta} f_j(a) da d\theta$ ,  $\mathbf{R} = \text{diag}\{R_1, R_2, \dots, R_N\}$ .

## Results

To give an example, an extensive literature survey was performed and provided us with just one set of data (6)

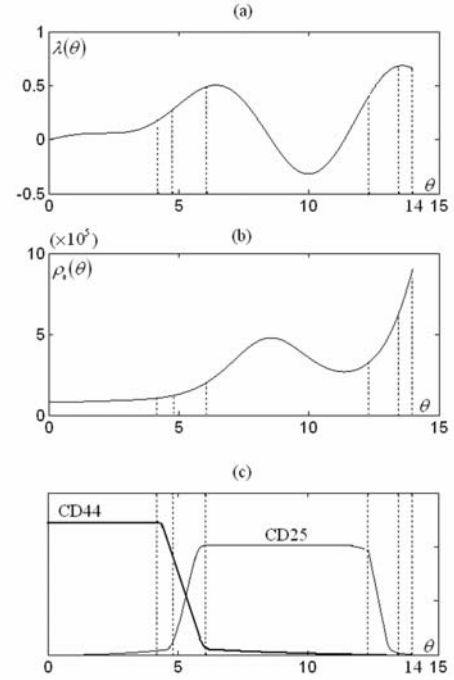


Figure 4. (a) and (b) show the obtained  $\lambda(\theta)$  and  $\varrho_0(\theta)$  by using data from (6) and  $I_0 = 8.075 \times 10^4$ . (c) shows the expression profile of CD44 (thick line) and CD25 (thin line). The dotted lines show the delimitations between subsets.

which appears sufficient. The data were obtained from a healthy mouse and described exclusively the DN compartment. DN thymocytes were divided into  $N=6$  subsets, namely  $\text{CD44}^+ \text{CD25}^-$  (DN1),  $\text{CD44}^+ \text{CD25}^{\text{low}}$  (DN2),  $\text{CD44}^+ \text{CD25}^{\text{high}}$  (DN3),  $\text{CD44}^- \text{CD25}^{\text{high}}$  (DN4),  $\text{CD44}^- \text{CD25}^{\text{low}}$  (DN5),  $\text{CD44}^- \text{CD25}^-$  (DN6). Besides  $S_i$ , for each subset they measured  $\eta_i$  (the percentage of the cycling cells) that can be converted to  $\bar{\lambda}_i^p$  according to  $\lambda_i^p = \eta_i \ln 2/T$  where  $T=9 \sim 10$  hour (7) is the cycle time of the thymocyte mitosis (we use  $T=9.5$  hour  $= 0.396$  day). Many studies (e.g., (8)) show that the baseline death level of the DN cells is very low and can be ignored. However, the death in DN4 subset is considerable and was estimated to be about 70% of the corresponding proliferation (6), namely  $\bar{\lambda}_4^a \approx 0.7 \bar{\lambda}_4^p$ . Other  $\lambda_i^a$  values ( $i=1,2,3,5,6$ ) are simply assumed as 0. For the present case of normal, unmanipulated thymus, was estimated to be between  $5 \times 10^4$  and  $5 \times 10^5$  (7).

The Whittaker's Cardinal Function (9)  $f_j(\theta) = \text{sinc}(\pi(\theta - j\Delta/\Delta))$  (we use  $\Delta=3$ ) is chosen as the basis function. By performing the computation using  $I_0 = 5 \times 10^4$ ,  $\mathbf{x}$  is promptly obtained (The root-finding converges in only 21 iterations and is quite fast). In particular the value of  $\theta_6$  (represents the length of the DN stage) is 18.06, which is close to 14, the generally accepted value (10). After several trial-and-error runs,  $\theta_6$  is accurately tuned to 14 by choosing  $I_0 = 8.075 \times 10^4$ . The result is shown in Figure 4. The duration of each stage  $\theta_i - \theta_{i-1}$  is 4.21, 0.56, 1.31, 6.23, 1.15, and 0.54 days,

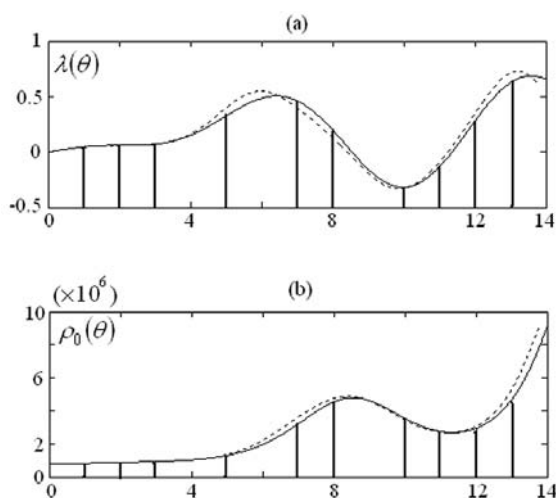


Figure 5.  $\lambda(\theta)$  and  $\rho_0(\theta)$  obtained by the first approximation are shown in dotted lines and that obtained by both steps are shown in solid thin lines. The thin lines show the delimitations of the 11 re-defined subsets.

respectively. These parameters, to the best of our knowledge, have not yet been determined by other researchers. The profile of CD44 and CD25 expressions is shown in Figure 4(c). As one can see, up- and down-regulation steps are fast processes, as indicated by the short periods of the DN<sub>2,3,5,6</sub> stages. DN<sub>4</sub> is the longest, which implies that some complex process may be involved. Indeed, at this stage most of the cells display the hallmark of irreversible immunological commitment to the T lineage in the form of TCR  $\beta$ -gene rearrangements (6,10). The process may generate out-of-frame TCR  $\beta$ -chains that are unresponsive to adequate stimulation; cells carrying such pre-TCRs will subsequently die. This may well be the reason why  $\lambda(\theta)$  has a negative part in the DN<sub>4</sub> stage as shown in Figure 4(a). The simplified process inferred from Figure 4 is as follows. The early cells receive little stimulation and the proliferation increases steadily as the cells mature (This again corresponds well to the biological facts. The progenitors enter the thymus at the cortico-medullary junction where few stimulating thymic epithelial cells reside; as they migrate to the outer cortex, more and more epithelial cells show up and secrete cytokines to stimulate proliferation). At the DN<sub>4</sub> stage, TCR rearrangement begins and many unselected cells die. This pushes the otherwise escalating growth rate down below zero. It subsequently increases again driving the cells to other stages. From Figure 4(b) one reads that each day there are about  $9.05 \times 10^5$  cells emigrating from the DN compartment.

**Discussion**

T cell differentiation constitutes one of the basic and most vital processes in immunology. A good conceptual framework

is essential to reduce the enormously complicated process to a realistic biophysical model that can provide insights leading to new theories and discovery. In this paper such a model has been constructed. The partial differential structure allows a continuous description of the thymocyte maturation, which opens a window for probing into the microscopic world of T cell differentiation. The computation is quite easy. The first approximation involves only an inversion of the matrix Q, which takes little time even if N is very large. Furthermore, the larger N is, the closer is to the actual solution x (the trapezoid approximation is more accurate as the subsets are more narrowly divided), and the easier the subsequent root-finding will be. To show this, the  $\theta$ -axis of Figure 4 is re-divided into  $N=11$  parts and the data set  $\mathbf{d}=[S_1, S_2, \dots, S_{11}, \bar{\lambda}_1, \bar{\lambda}_2, \dots, \bar{\lambda}_{11}]$  is then calculated to be used as the "artificial data." The reconstructed  $\lambda(\theta)$  and  $\rho_0(\theta)$  obtained by the first approximation only and obtained by both steps are shown in Figure 5 as dotted lines and solid lines, respectively. One sees that they are very close. The root-finding only takes 5 iterations. The methods also apply to other stages of T cell differentiation. In future, by finely dividing the thymus and collecting more data, a very detailed  $\lambda(\theta)$  can be obtained without any computational difficulty.

The model provides an ideal framework for studying lymphomagenesis, since pathological evolution  $\varrho(\theta, t)$  can be obtained by integrating Eq. (I) with perturbed  $\lambda(\theta)$  and  $\mu(\theta)$ , which represent disturbed growth and differentiation factors.

**References**

- 1 Ritter MA, and Crispe IN: The Thymus. Oxford University Press, Oxford, 1992.
- 2 Poo WJ, Conrad L and Janeway Jr CA: Receptor-directed focusing of lymphokine release by helper T cells. Nature 332: 378-380, 1988.
- 3 Mehr R, Globerson A, and Perelson AS: Modeling positive and negative selection and differentiation processes in the thymus. J Theor Biol 175: 103-126, 1995.
- 4 Mehr R, Perelson AS, Fridkis-Harell M and Globerson A: Feedback regulation of T cell development in the thymus. J Theor Biol 181: 157-167, 1996.
- 5 Press WH, Flannery BP, Teukolsky SA and Vetterling WT: Numerical Recipes. Cambridge University Press, 1986.
- 6 Pénit C, Lucas B and Vasseur F: Cell expansion and growth arrest phases during the transition from precursor (CD4-8-) to immature (CD4+8+) thymocytes in normal and genetically modified mice. J Immunol 154: 5103-5113, 1995.
- 7 Pénit C, Vasseur F and Papiernik M: In vivo dynamics of CD4-8-thymocytes: Proliferation, renewal and differentiation of different cell subsets studied by DNA biosynthetic labeling and surface antigen detection. Eur J Immunol 18:1343-1350, 1988.
- 8 Adkins B, Charyulu V, Sun QL, Lobo D and Lopez DM: Early block in maturation is associated with thymic involution in mammary tumor-bearing mice. J Immunol 164: 5635-5640, 2000.
- 9 McNamee J, Stenger F and Whidney EL: Whittaker's cardinal function in retrospect. Math Comput 25: 141-154, 1971.
- 10 Petrie HT: Role of thymic organ structure and stromal composition in steady-state postnatal T-cell production. Immunol Rev 189: 8-19, 2002.

Received January 13, 2004